Modeling Drug-Induced Hepatic Fibrosis *In Vitro* Using Three-Dimensional Liver Tissue Constructs

THE UNIVERSITY of NORTH CAROLINA® at CHAPEL HILL

Leah M. Norona[1,2], Deborah G. Nguyen[3], David A. Gerber[1], Sharon C. Presnell[3], Edward L. LeCluyse[1,2] | [1]The University of North Carolina at Chapel Hill, Chapel Hill, NC, [2]The Hamner Institutes, Research Triangle Park, NC, [3]Organovo, Inc., San Diego, CA

Introduction

While the major precipitating factors underlying drug- and chemical-induced fibrosis have been gleaned from animal models, the key initiating and series of adaptive events that perpetuate this response, especially in humans, are still not well understood. Regardless of etiology, progressive fibrotic liver injury is orchestrated by complex intercellular interactions among hepatocytes (HCs), endothelial cells (ECs), hepatic stellate cells (HSCs), Kupffer cells (KCs) and recruited bone-marrow derived cells. This interplay between resident and recruited cell types results in the appearance and progression of disease features that are best detected and interpreted in the context of a three-dimensional (3D) tissue environment, including inflammation, fibrogenesis, tissue remodeling, and compensatory hepatocellular regeneration.

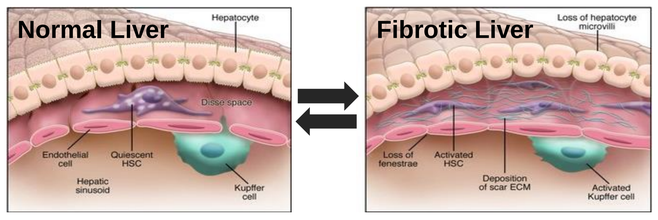

Adapted from: Iredale, J.P., J Clin Invest. (2007) 117(3): 539-548.

The recent availability of human liver tissue models (Fig. 1) that incorporate both parenchymal (*i.e.*, HCs) and non-parenchymal cells (*i.e.*, HSCs and ECs) in a three-dimensional context has created the opportunity to examine progressive liver injury in response to known pro-fibrotic modulators. Here we demonstrate the utility of 3D bioprinted tissues to perform more in-depth evaluation of compound-induced liver fibrosis in an *in vitro* setting.

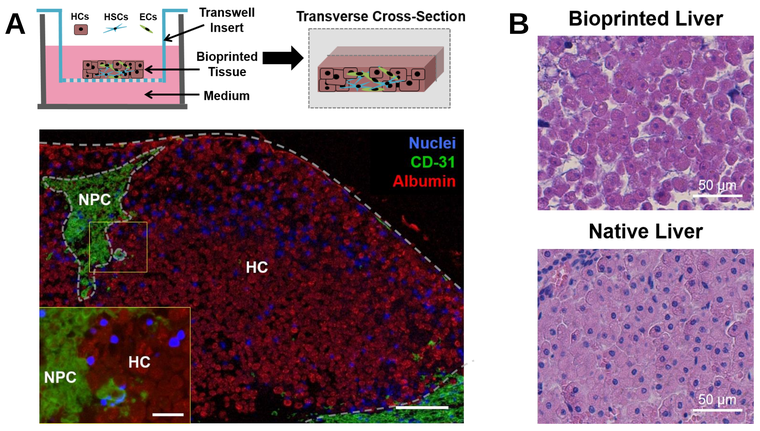

Figure 1: 3D bioprinted tissue recapitulates the tissue-like density of native liver. Transverse cross-section of bioprinted liver tissue with compartmentalized architecture (A; outlined) as depicted with CD-31 and albumin as markers of the non-parenchymal (NPC) and parenchymal or hepatocellular (HC) compartments, respectively. Inset scale bar = 25 µm. Scale bar = 100 µm. Comparison of Hematoxylin and Eosin (H&E) stained native liver and bioprinted liver (B). The 3D context of bioprinted liver and incorporation of non-parenchymal cells (*i.e.*, HSCs and ECs) support normal liver function and maintain phenotypic features of cells for at least 42 days.

Methods

Standard ExVive3D™ Liver Tissues were manufactured and provided by Organovo (San Diego, CA).

Maintenance and Compound Exposure. Tissues were maintained in exVive3D™ Liver culture medium provided by Organovo (San Diego, CA) for 3 days prior to compound exposure. Exposure to vehicle (0.1% DMSO), fibrogenic drug methotrexate (MTX; 0.1 or 1.0 µM), or prototypical fibrogenic agent thioacetamide (TAA; 5.0 or 25 mM) occurred daily for 7 or 14 days.

***Goal:** Mimic the onset of compound-induced hepatic fibrosis in exVive3D™ Liver using classified fibrogenic agents.*

Summary

- **ExVive3D™ bioprinted liver tissue represents a unique platform for measuring the effects of repeated compound exposure.**
- **Bioprinted liver tissues can recapitulate in part the cellular, molecular, and histopathological events associated with drug-, chemical-, and TGF-β1-induced fibrogenesis.**
- **This novel model system may lead to a better understanding of the early key events underlying chronic liver injury leading to fibrosis in humans and the classification of fibrogenic agents for risk assessment purposes.**

Results

Physiologically relevant concentrations of select agents allow us to model conditions that favor fibrogenesis

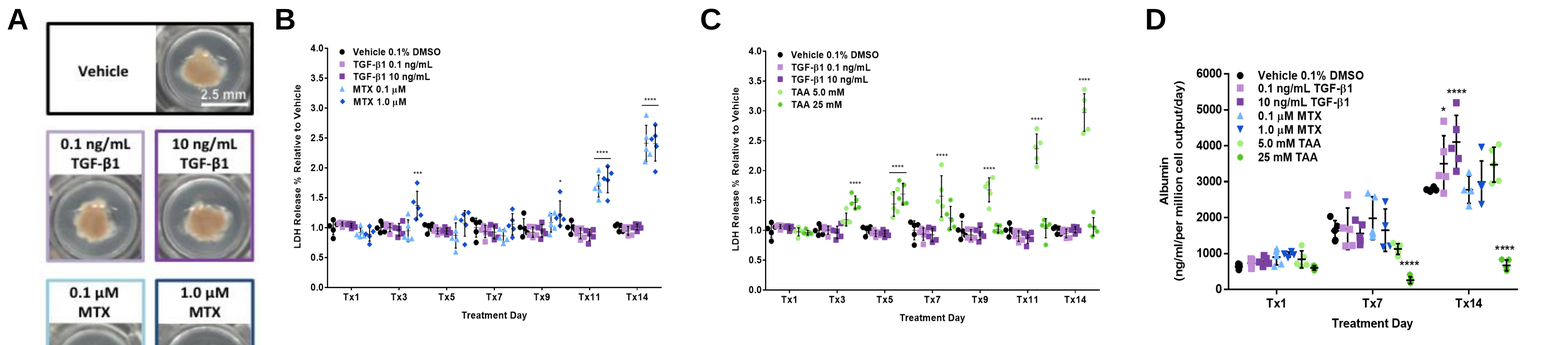

Figure 2: Impact of fibrotic agents on bioprinted liver tissue viability and functionality. Gross images of tissues following 14 days of treatment (A). Extended 14-day treatment with MTX (B) and TAA (C) resulted in tissue damage, as evidenced by significant increases in LDH release (n = 9 for Tx1-Tx7, n = 5 for Tx9-Tx14) . Conversely, no overt damage is observed with TGF treatment. The degree of hepatocellular damage as measured by albumin output (D; n = 5) at key time points during the treatment period was most pronounced with 25 mM TAA, as demonstrated by a statistically significant decrease in albumin output relative to vehicle treated control. Significance was determined using a one-way ANOVA with post hoc Dunnett's multiple comparisons test (**p*<0.05, ***p*<0.01, ****p*<0.001, *****p*<0.0001).

Histological examination reveals key features of clinical fibrosis in bioprinted tissues following 14 days of treatment with select fibrogenic agents

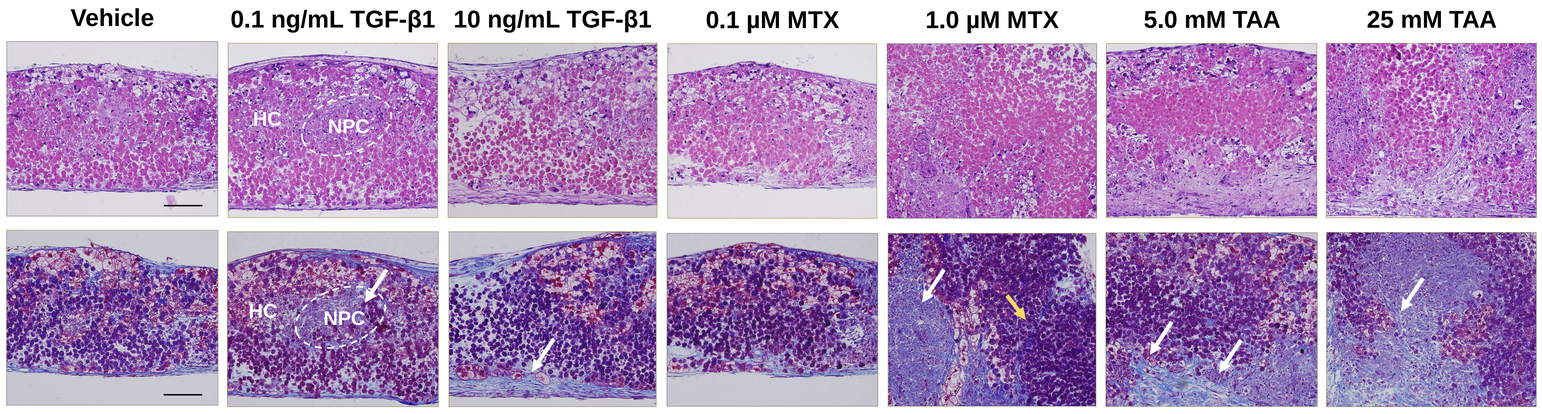

Figure 3: Histological assessment of bioprinted liver. Fixed tissues sections were stained with H&E to examine tissue architecture (above, top panel). Additional cross-sections were stained with Gomori's One-Step trichrome (above, bottom panel) to visualize collagen (blue), cytoplasm (pink/purple), and nuclei (dark purple). TGF treatment caused focal nodular fibrosis (white arrows) in the NPC compartment but generally preserved HC mass. MTX caused mild hepatocellular damage and nodular and pericellular fibrosis at lower doses, with evidence of bridging fibrosis (yellow arrow) at 1.0 µM. Treatment with TAA nearly eliminated HCs in the tissues by 14 days, with the majority of tissue replaced by fibrotic scar tissue. Scale bar = 100 µm. Additional tissues were assessed to gauge the composition and distribution of specific collagen subtypes (right). Collagen I positive areas are localized to regions of fibrillar ECM at the apical (white arrow) and basolateral (yellow arrow) edges of the tissue as well as areas with extensive ECM accumulation (outlined) and nodular areas of collagen deposition (NF). Collagen IV was mainly localized to the periphery of hepatocytes. Vimentin exhibited treatment-dependent differences in patterning and distribution with the transition of punctate areas of vimentin positivity (white arrows) to a more diffuse appearance (yellow arrows) and localization to areas associated with extensive ECM deposition (NF). The black and white inset (100%) in each photomicrograph highlights the shift in vimentin patterning observed with treatment. Scale bar = 25 µm.

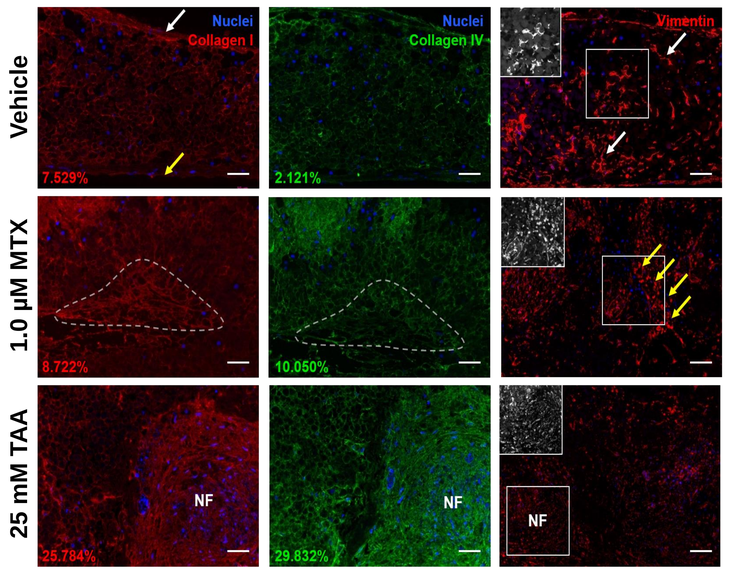

Initial insight into other fibrogenic parameters suggest tissues are in an active state of wound healing

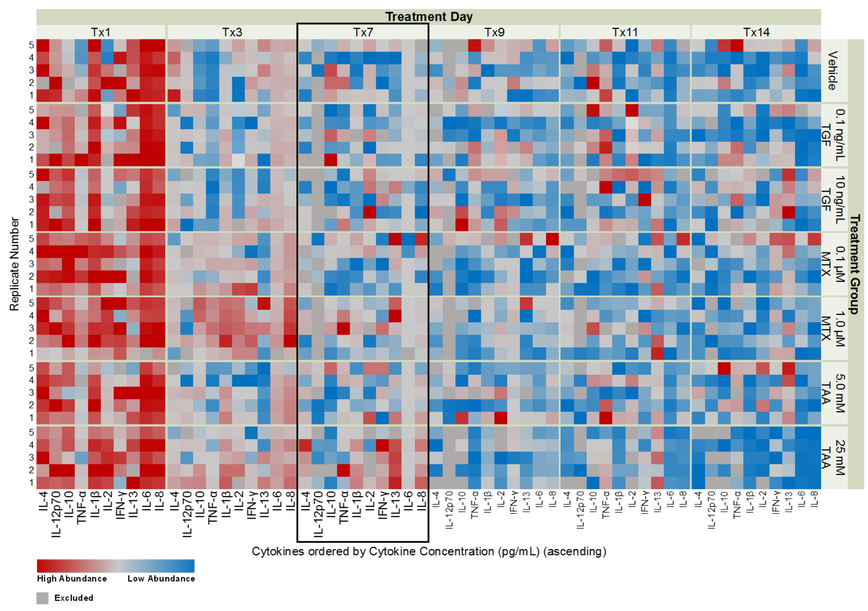

Figure 4: Abundance of cytokines released into the culture medium over the treatment time course. The prevalence of proinflammatory cytokines (pg/mL) declines over time towards steady-state levels by Tx7 (above). Measurement of cytokine levels at Tx7 and Tx14 (n = 5) showed treatment- and time-dependent differences in immunomodulatory and chemotactic cytokines (right). IL-6 regulates acute phase response proteins in response to injury and was significantly increased at Tx7 for 1.0 µM MTX and both TAA treatment groups. Monocyte chemotactic protein-1 (MCP-1), involved in facilitating macrophage/monocyte infiltration to perpetuate an adaptive response to continued insult, increased at Tx14 for MTX and TAA treatment. Significance was determined using a one-way ANOVA with post hoc Dunnett's multiple comparisons test (**p*<0.05, ***p*<0.01, ****p*<0.001, *****p*<0.0001).

Treatment	Day 7		Day 14	
	ACTA2	*COL1A1*	*ACTA2*	*COL1A1*
Vehicle	1.000 ± 0.062	1.000 ± 0.232	1.000 ± 0.103	1.000 ± 0.092
0.1 ng/mL TGF-β1	1.090 ± 0.064	1.165 ± 0.081	0.968 ± 0.002	1.098 ± 0.403
10 ng/mL TGF-β1	-	-	1.717 ± 0.054	1.842 ± 0.053
0.1 µM MTX	1.427 ± 0.092	1.415 ± 0.040	2.227 ± 0.055	2.054 ± 0.243
1.0 µM MTX	1.355 ± 0.291	1.155 ± 0.208	2.107 ± 0.149	2.596 ± 0.223
5.0 mM TAA	-	-	2.056 ± 0.318	1.636 ± 0.292
15 mM TAA	-	-	*	1.086 ± 0.190

Values are the means ± SD (n = 2), shaded values denote a fold-change greater than 2 relative to time-matched vehicle. *Denotes average fold change of 0.0004

Table 1: Time-dependent up-regulation of two fibrosis-associated genes. The levels of fibrogenic markers α-smooth muscle actin (ACTA2) and collagen, type 1, α1 (COL1A1) were measured using RNA isolated from whole tissue constructs. Values are represented as fold-change relative to vehicle control. Treatment-induced induction of these genes suggests active fibrogenic processes and provide evidence to support collagen deposition within the tissue constructs.

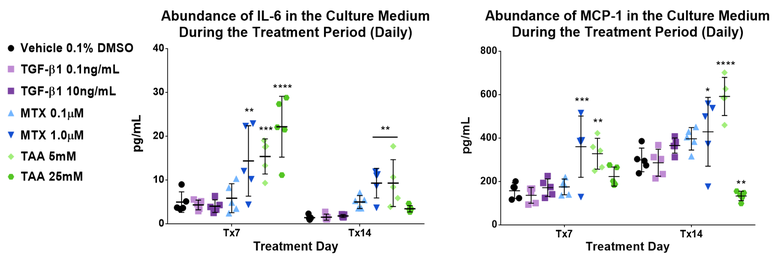

Funding/Support:

R25 GM055336, IMSD Fellowship, NIH, Virginia L. Miller, PI
T32 ES007126, Pre- and Postdoctoral Training in Toxicology, NIEHS, Ilona Jaspers, PI